Unified Registration Framework for Cumulative Dose Assessment in Cervical Cancer across External Beam Radiotherapy and Brachytherapy

Sharmili Roy[a], John J. Totman[a], and Bok A. Choo[b]

[a]A*Star-NUS Clinical Imaging Research Centre, Singapore
[b]National University Cancer Institute, Singapore

ABSTRACT

Dose accumulation across External Beam Radiotherapy (EBRT) and Brachytherapy (BT) treatment fractions in cervical cancer is extremely challenging due to structural dissimilarities and large inter-fractional anatomic deformations between the EBRT and BT images. The brachytherapy applicator and the bladder balloon, present only in the BT images, introduce missing structural correspondences for the underlying registration problem. Complex anatomical deformations caused by the applicator and the balloon, different rectum and bladder filling and tumor shrinkage compound the registration difficulties. Conventional free-form registration methods struggle to handle such topological differences. In this paper, we propose a registration pipeline that first transforms the original images to their distance maps based on segmentations of critical organs and then performs non-linear registration of the distance maps. The resulting dense deformation field is then used to transform the original anatomical image. The registration accuracy is evaluated on 27 image pairs from stage 2B−4A cervical cancer patients. The algorithm reaches a Hausdorff distance of close to 0.5 mm for the uterus, 2.2 mm for the bladder and 1.7 mm for the rectum when applied to (EBRT,BT) pairs, taken at time points more than three months apart. This generalized model-free framework can be used to register any combination of EBRT and BT images as opposed to methods in the literature that are tuned for either only (BT,BT) pair, or only (EBRT,EBRT) pair or only (BT,EBRT) pair. A unified framework for 3D dose accumulation across multiple EBRT and BT fractions is proposed to facilitate adaptive personalized radiation therapy.

Keywords: Geodesic distance-based registration, brachytherapy, dose accumulation

1. INTRODUCTION

Cervical cancer responds well to radiotherapy. Standard treatment for locally advanced cervical cancer (FIGO stage 2B−4A) is concurrent weekly chemotherapy, external beam radiotherapy (EBRT) and high-dose-rate (HDR) brachytherapy (BT). HDR brachytherapy, often in multiple fractions, is used to boost EBRT [1]. Treatment outcome is greatly influenced by organ doses over multiple treatment fractions [2,3,4]. Treatment evaluation should consider the combined EBRT and BT dose in each tissue. However, in current clinical practice, EBRT and BT fractions are optimized individually which results in multiple dose distributions associated with their corresponding anatomical images. These anatomical images are acquired at different time points and exhibit large deviations in the patient's anatomy. A crucial step towards estimating the accumulated dose across multiple fractions is to accurately register the underlying anatomical images [5]. This registration is very challenging due to many reasons. The brachytherapy applicator and the bladder balloon, present only in the BT image, introduces structural dissimilarities between EBRT and BT images. The applicator and the balloon introduce complex anatomical deformations in the uterus, bladder and the surrounding organs. Different rectum and bladder filling and tumor shrinkage over the course of the treatment are also factors that compound registration difficulties.

A recent study aiming to map EBRT dose distribution to BT MRIs using an intensity-based non-rigid registration available on a commercial software report that registration failed in six out of 15 patients due to 'unreasonable' anatomical deformations [5]. Four major approaches have been proposed in the literature that

Send all correspondence to: Sharmili Roy, E-mail: sharmili@nuhs.edu.sg

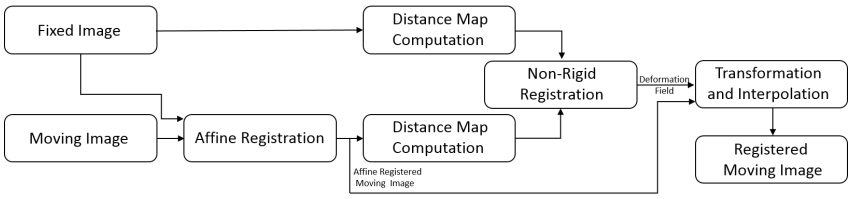

Figure 1. Overview of the registration pipeline.

address dose accumulation across EBRT and BT fractions or across multiple BT fractions using customized registration procedures [2,6,7,8]. One of the first attempts to solve this problem was to use viscous fluid model to transform the EBRT image to the BT image [2]. No bio-mechanical modeling of the tissues was performed and multiple registrations were sometimes required to get acceptable results. Recently, Berendsen et al. proposed a geometric penalty-based registration that matches BT to EBRT image by folding the applicator region and bringing the applicator volume down to zero [6]. This assumes that an accurate applicator model is available. Folding the applicator results in folding inside the uterus. Also, assuming that an applicator model would be available in all cases is not feasible. Prior to therapy, applicators are typically chosen and set up according to the size of a patients uterus/cervix. Creating a model of the applicator before each fraction is clinically impractical. Osorio et al. segment various features surrounding the critical organs and then individually register each pair of features and each pair of critical organs [7]. A final deformation vector is obtained by combining all individual registrations. Since there is no regularization that constraints the individual transformations to be coherent, the resulting deformation is not guaranteed to be bijective. Also, this algorithm takes about 86 minutes to register one image pair. In another work Zhen et al. register two BT images by first segmenting the applicator region in both the images and then matching surface points on the cavity left by the segmented applicators [8]. This method is tuned towards precisely matching the applicator region. Registration results for the whole uterus and the surrounding critical organs are not reported. Some methods are tuned to registering only (EBRT,EBRT) pairs, some tuned to only (BT,BT) pairs and some only to (EBRT,BT) pairs. None of these methods handle registrations for all combinations of EBRT and BT images and hence cannot accumulate dose across multiple EBRT and BT fractions. The goal in this paper is to design a unified registration framework that can be used to register any combination of EBRT and BT images for a cumulative dose assessment throughout the course of the treatment.

2. METHODS

The proposed method is designed to work on a data set where EBRT and BT images of a patient are acquired at different sites and in scanners that have different field strengths and scanning protocols. This makes using intensity-based methods all the more ineffectual. To overcome different acquisition protocols and structural differences between EBRT and BT images posed by the brachytherapy applicator and the bladder balloon, the proposed registration framework first transforms the anatomical images into their distance maps based on segmentations of critical organs and then registers the distance maps using a non-rigid registration. The deformation resulting from this registration is then used to transform the original anatomical image. Figure 1 shows the overall registration pipeline. In line with similar works in the literature, prior information in terms of segmentations of the critical organs are assumed to be available [2,7].

2.1 Geodesic distance computation

Use of unsigned geodesic distances is proposed for computation of the distance maps. Geodesic distances take into account image gradients and define distances using the shortest path along the image intensities rather than using flat physical distances. Given a 3D image I, an anatomical region Ω, and a binary mask M (with $M(\boldsymbol{x}) \in \{0,1\}\ \forall \boldsymbol{x}$) such that $\boldsymbol{x} \in \Omega \iff M(\boldsymbol{x}) = 0$, the unsigned geodesic distance of each pixel $\boldsymbol{x}$ from Ω is defined as:

$$D(\boldsymbol{x}; M, \triangledown I) = \min_{\{\boldsymbol{x}' | M(\boldsymbol{x}')=0\}} d(\boldsymbol{x}, \boldsymbol{x}') \tag{1}$$

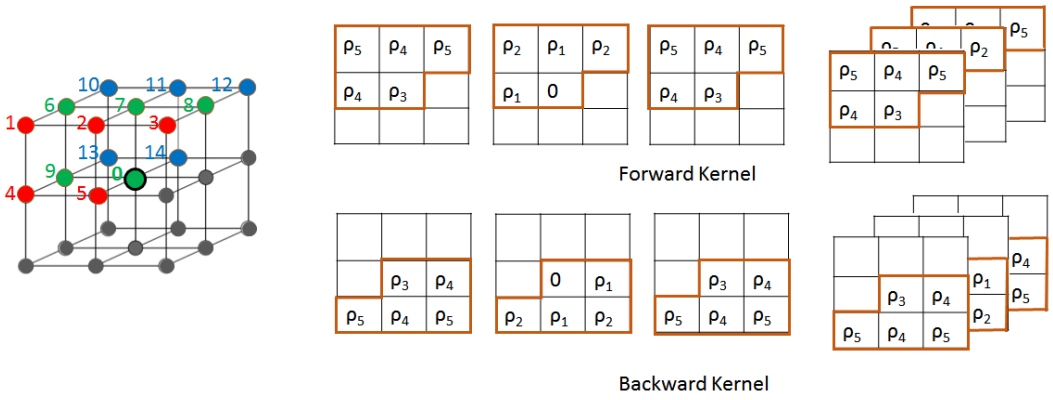

Figure 2. Kernel for 3D geodesic distance transform.

$$d(\mathbf{a},\mathbf{b}) = \min_{\mathbf{\Gamma}\in\mathcal{P}_{\mathbf{a},\mathbf{b}}} \int_0^1 \sqrt{||\mathbf{\Gamma}'(s)||^2 + \gamma^2(\nabla I \cdot \mathbf{u})}\ ds \tag{2}$$

with $\mathcal{P}_{\mathbf{a},\mathbf{b}}$ being the set of all paths between points $\mathbf{a}$ and $\mathbf{b}$. $\mathbf{\Gamma}(s)\colon \Re \to \Re^2$ is one such path parametrized by its arclength $s \in [0,1]$. The spatial derivative $\mathbf{\Gamma}'(s)$ is defined as $\mathbf{\Gamma}'(s) = \partial\mathbf{\Gamma}(s)/\partial s$. The unit vector $\boldsymbol{u} = \mathbf{\Gamma}'(s)/||\mathbf{\Gamma}'(s)||$ is tangent to the direction of the path. γ weighs the image gradient contribution against the physical distances. For $\gamma = 0, D$ reduces to Euclidean distance. This work proposes that the geodesic distance of a voxel from a critical organ should remain approximately constant in the two images being registered even though the physical location of the voxel does not remain constant.

Two main kinds of algorithms are described in the literature to compute geodesic distances: *raster-scan* and *wave-front propagation*. Raster-scan algorithms are based on kernel operations applied sequentially over the image in multiple passes [9]. On the other hand, wave-front algorithms such as Fast Marching Methods (FMM) are based on iterative propagation of a pixel front with velocity F [10]. FNM requires accessing image locations far from each other in memory thus limiting the speed of execution. Raster-scan technique, on the other hand, accesses the image memory in contiguous blocks, thus reducing memory access delays. This paper uses raster-scan technique briefly described below [9].

Given a map $M(\boldsymbol{x}) \in [0,1]$, the map is scanned with a $3 \times 3 \times 3$ kernel from top-left-front to the bottom-right-back corner in the forward pass and an intermediate function $C(\boldsymbol{x})$ is iteratively computed as defined in Equation 3 and illustrated in Figure 2.

$$C(x,y,z) = min \begin{cases} C(x-1,y-1,z-1) + \sqrt{\rho_5 + \gamma\nabla I_{1,0}(x,y,z)^2} \\ C(x,y-1,z-1) + \sqrt{\rho_4 + \gamma\nabla I_{2,0}(x,y,z)^2} \\ C(x+1,y-1,z-1) + \sqrt{\rho_5 + \gamma\nabla I_{3,0}(x,y,z)^2} \\ C(x-1,y,z-1) + \sqrt{\rho_4 + \gamma\nabla I_{4,0}(x,y,z)^2} \\ C(x-1,y-1,z) + \sqrt{\rho_2 + \gamma\nabla I_{6,0}(x,y,z)^2} \\ C(x,y-1,z) + \sqrt{\rho_1 + \gamma\nabla I_{7,0}(x,y,z)^2} \\ C(x+1,y-1,z) + \sqrt{\rho_2 + \gamma\nabla I_{8,0}(x,y,z)^2} \\ C(x-1,y,z) + \sqrt{\rho_1 + \gamma\nabla I_{9,0}(x,y,z)^2} \\ C(x-1,y-1,z+1) + \sqrt{\rho_5 + \gamma\nabla I_{10,0}(x,y,z)^2} \\ C(x,y-1,z+1) + \sqrt{\rho_4 + \gamma\nabla I_{12,0}(x,y,z)^2} \\ C(x+1,y-1,z+1) + \sqrt{\rho_5 + \gamma\nabla I_{13,0}(x,y,z)^2} \\ C(x-1,y,z+1) + \sqrt{\rho_4 + \gamma\nabla I_{14,0}(x,y,z)^2} \\ \nu M(x,y,z) \end{cases} \tag{3}$$

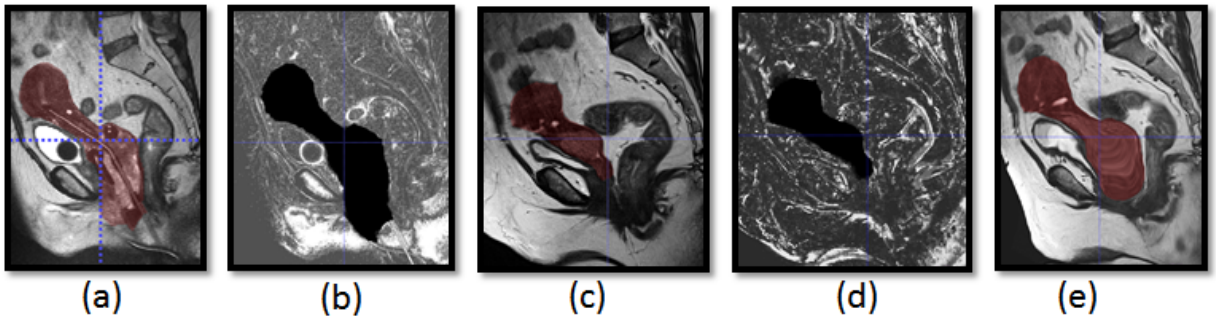

Figure 3. (a) BT image with overlaid uterus segmentation, (b) uterus-based geodesic distance map of BT image, (c) EBRT image with overlaid uterus segmentation, (d) uterus-based geodesic distance map of EBRT image, (e) EBRT image registered to BT image based on registration of (b) and (d).

The image gradients, ∇I's, are computed using the directions highlighted in Figure 2. For example, $\nabla I_{7,0}$, is the gradient in the north direction. The ρ_i's are the local distances. The ρ_1 and ρ_2 are the in-plane distances and are normalized to 1 and $\sqrt{2}$ respectively. The ρ_3 depends on the out-of-plane distance. The ρ_4 and ρ_5 are set based on ρ_3 and the corresponding triangular geometry. The algorithm runs from the bottom-right-back to the top-left-front corner and applies the backward kernel to $C(\boldsymbol{x})$. This generates the final distance $D(\boldsymbol{x})$ (Equation 1). Larger kernels approximate the exact distance better.

2.2 Deformable registration

The EBRT and BT images are first registered using an affine registration to align the bony anatomy. Geodesic distance maps are then computed for the registered images using uterus segmentation as the binary mask. The distance maps are smoothed using bilateral filtering. The distance maps are then non-linearly registered using a bspline-based registration. This registration is formulated with a similarity energy function comprising of mutual information [11] and a rigidity penalty [12]. Ten iterations of this registration are applied in a multi-resolution fashion where the control point spacing gradually reduces to eight voxels. Elastix toolbox is used to implement this registration scheme [13].

3. RESULTS

Registration accuracy is assessed on 27 image pairs from stage 2B−4A cervical cancer patients. The BT images are acquired on a 1.5T Magnetic Resonance (MR) machine and the EBRT are acquired on a 3T simultaneous positron emission technology/ magnetic resonance (PET/MR) machine. Figure 3 illustrates registration for a (EBRT,BT) pair. Geodesic distance-based registration is able to handle large deformations in the organ of interest, which is the uterus in this case. However, the probability of erroneous anatomical deformations increase as the distance from the organ surface increases.

Figure 4 shows the quantitative analysis of the registration accuracy using Dice score and Hausdorff distance on (EBRT,BT) pairs at time points more than three months apart. The scores are computed between segmentation of the fixed image and the transformed segmentation of the moving image. Geodesic distance is compared against conventional physical distances such as Euclidean, Cityblock, Chessboard and Quasi-Euclidean distances. Geodesic distance is found to be superior to the other distance metrics and to bspline-based non-rigid registration. The evaluation data set also includes a patient that had an anteverted (forward tilted) uterus which increases the complexity of deformation in the BT image and hence causes larger variation in registration accuracy. The baseline bspline-based non-rigid registration between the EBRT and BT images was implemented using mutual information similarity [12] and a rigidity penalty [12].

Figure 5 shows registration results for (BT,BT) and (EBRT,EBRT) pairs. Geodesic distances clearly give better registration results for the uterus. Since (BT,BT) and (EBRT,EBRT) pairs preserve underlying structural correspondences, bspline-based non-linear registration sometimes aligns the bladder and the rectum more accurately.

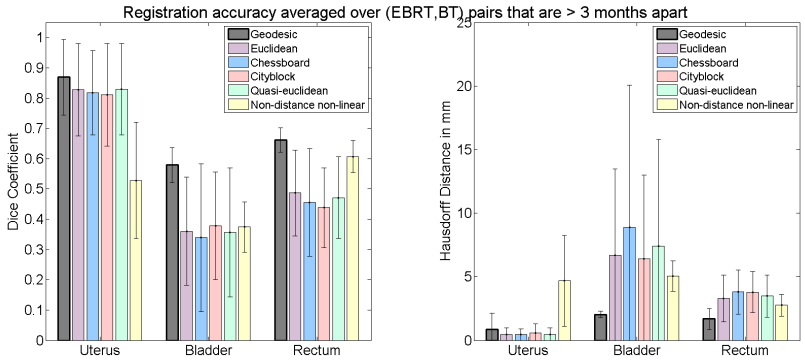

Figure 4. Comparative analysis of registration accuracy for Geodesic distance-based registration with respect to other distance metrics and conventional free-form registration for (EBRT,BT) pairs.

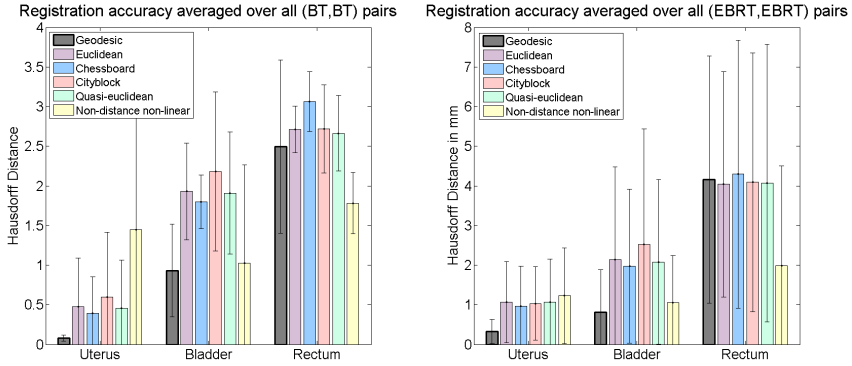

Figure 5. Comparative analysis of registration accuracy for (BT,BT) pairs and (EBRT,EBRT) pairs.

4. DISCUSSION

It is observed that the registration accuracy of the uterus is high using the proposed approach. However, the accuracy of registration of the bladder is lower. This is mainly due to the presence of the bladder balloon in the BT image which results in very complex deformations in the bladder. In future, we aim to overcome the lower registration accuracy of the bladder and the rectum using a multi-distance map based approach. This approach will compute three distance maps, one each from the uterus, bladder and the rectum. Registration based on these distance maps will be computed along with a background non-linear registration. A final fusion of the deformation would be done to achieve high accuracy in all the three organs of interest.

The proposed method assumes prior segmentation of the uterus. Typically in MRI-guided radiation therapy planning for cervical cancer, the tumor, cervix, vagina, parametria, uterus, bladder and rectum are contoured in MRI by a radiation therapist [14]. In theory, these contours can be used for registration if accessible. Further, in future we plan to study the sensitivity of the proposed registration to segmentation accuracy and investigate if an semi-automated/automated rough segmentation will give reasonable registration results.

5. CONCLUSIONS

This paper addresses the problem of registering brachytherapy and external beam radiotherapy MRIs of the pelvis for quantifying dose accumulation in each organ. The deformations present in the images are too high for traditional deformable registration methods. The paper proposes to use geodesic distance maps that can be more robustly registered than the original images. This effectively simplifies the challenging registration problem and allows to register a pair of external beam radiotherapy images or a pair of brachytherapy images or

a combination of external beam radiotherapy and brachytherapy images within the same framework. Hence, the proposed framework can be used for a cumulative 3D dose accumulation assessment across multiple fractions of external beam radiotherapy and brachytherapy. This strives to pave the way for making adaptive personalized radiation therapy for cervical cancer patients a possibility.

ACKNOWLEDGMENTS

This work has been partially funded by the NMRC NUHS Centre Grant - Medical Image Analysis Core (NMRC/CG/013/2013).

REFERENCES

[1] Han, K., Milosevic, M., Fyles, A., Pintilie, M., and Viswanathan, A. N., "Trends in the utilization of brachytherapy in cervical cancer in the united states," *International Journal of Radiation Oncology* Biology* Physics* **87**(1), 111–119 (2013).

[2] Christensen, G. E., Carlson, B., Chao, K. C., Yin, P., Grigsby, P. W., Nguyen, K., Dempsey, J. F., Lerma, F. A., Bae, K. T., Vannier, M. W., et al., "Image-based dose planning of intracavitary brachytherapy: registration of serial-imaging studies using deformable anatomic templates," *International Journal of Radiation Oncology* Biology* Physics* **51**(1), 227–243 (2001).

[3] Osorio, E. M. V., Hoogeman, M. S., Teguh, D. N., Al-Mamgani, A., Kolkman-Deurloo, I.-K. K., Bondar, L., Levendag, P. C., and Heijmen, B. J., "Three-dimensional dose addition of external beam radiotherapy and brachytherapy for oropharyngeal patients using nonrigid registration," *International Journal of Radiation Oncology* Biology* Physics* **80**(4), 1268–1277 (2011).

[4] Sabater, S., Andres, I., Sevillano, M., Berenguer, R., Machin-Hamalainen, S., and Arenas, M., "Dose accumulation during vaginal cuff brachytherapy based on rigid/deformable registration vs. single plan addition," *Brachytherapy* **13**(4), 343–351 (2014).

[5] Kim, H., Huq, M. S., Houser, C., Beriwal, S., and Michalski, D., "Mapping of dose distribution from IMRT onto MRI-guided high dose rate brachytherapy using deformable image registration for cervical cancer treatments: preliminary study with commercially available software," *J Contemp Brachytherapy* **6**(2), 178–184 (2014).

[6] Berendsen, F., Kotte, A., de Leeuw, A., Jürgenliemk-Schulz, I., Viergever, M., and Pluim, J., "Registration of structurally dissimilar images in MRI-based brachytherapy," *Physics in Medicine and Biology* **59**(15), 4033 (2014).

[7] Osorio, E. M. V., Kolkman-Deurloo, I.-K. K., Schuring-Pereira, M., Zolnay, A., Heijmen, B. J., and Hoogeman, M. S., "Improving anatomical mapping of complexly deformed anatomy for external beam radiotherapy and brachytherapy dose accumulation in cervical cancer," *Medical Physics* **42**(1), 206–220 (2015).

[8] Zhen, X., Chen, H., Yan, H., Zhou, L., Mell, L. K., Yashar, C. M., Jiang, S., Jia, X., Gu, X., and Cervino, L., "A segmentation and point-matching enhanced efficient deformable image registration method for dose accumulation between HDR CT images," *Physics in Medicine and Biology* **60**(7), 2981 (2015).

[9] Toivanen, P. J., "New geodosic distance transforms for gray-scale images," *Pattern Recognition Letters* **17**(5), 437–450 (1996).

[10] Yatziv, L., Bartesaghi, A., and Sapiro, G., "O(N) implementation of the fast marching algorithm," *Journal of Computational Physics* **212**(2), 393–399 (2006).

[11] Mattes, D., Haynor, D. R., Vesselle, H., Lewellyn, T. K., and Eubank, W., "Nonrigid multimodality image registration," in [*Medical Imaging 2001*], 1609–1620, International Society for Optics and Photonics (2001).

[12] Staring, M., Klein, S., and Pluim, J. P., "A rigidity penalty term for nonrigid registration," *Medical Physics* **34**(11), 4098–4108 (2007).

[13] Klein, S., Staring, M., Murphy, K., Viergever, M., Pluim, J. P., et al., "Elastix: a toolbox for intensity-based medical image registration," *Medical Imaging, IEEE Transactions on* **29**(1), 196–205 (2010).

[14] Ghose, S., Holloway, L., Lim, K., Chan, P., Veera, J., Vinod, S. K., Liney, G., Greer, P. B., and Dowling, J., "A review of segmentation and deformable registration methods applied to adaptive cervical cancer radiation therapy treatment planning," *Artificial Intelligence in Medicine* (2015).